FOREX Publication
Open Access | Rapid and quality publishing

International Journal of Electrical and Electronics Research (IJEER)
Research Article | Volume 12, Issue 2 | Pages 581-589 | e-ISSN: 2347-470X

Design, Fabrication and Performance Analysis of a Compact Unidirectional Quasi-Yagi Antenna for High Gain and High Directivity at 6.2 GHz

Nahid A Jahan[1], Ziaul Zafar[2] and Md. Asif Hossain[3]

[1]*Department of Electrical and Electronic Engineering, Southeast University, Bangladesh., nahid.jahan@seu.edu.bd*
[2]*Department of Electrical and Electronic Engineering, University of Dhaka, Bangladesh., zafarziaul@gmail.com*
[3]*Department of Electrical and Electronic Engineering, Southeast University, Bangladesh., asif.hossain@seu.edu.bd*

***Correspondence:** nahid.jahan@seu.edu.bd*

ABSTRACT- Antenna gain, directivity, and radiation efficiency are being enhanced by researchers to satisfy the demands of emerging mobile communication systems. Primarily, the quasi-Yagi antenna satisfies the expanded criterion. This study presents a microstrip quasi-Yagi antenna operating at 6.2 GHz. Enhancements are made to the antenna's gain, directivity, and radiation efficacy. At 6.2 GHz, the antenna was engineered to have a return loss S11 of -36 dB. In addition, from 5.85 to 6.4 GHz, -10 dB return loss was incorporated into its design. The Computer Simulation Technology (CST) Studio Suite was used to create this design. On a Rogers 3003 substrate, the improved design was manufactured.

Keywords: Quasi-Yagi Antenna; Microstrip Antenna; Antenna Fabrication and Design; Vector Network Analyzer; Wireless Communication.

ARTICLE INFORMATION

Author(s): Nahid A Jahan, Ziaul Zafar and Md. Asif Hossain;
Received: 05-04-2023; **Accepted**: 22-05-24; **Published**: 20-06-2024;
E- ISSN: 2347-470X;
Paper Id: IJEER230416;
Citation: 10.37391/ijeer-120233
Webpage-link:
https://ijeer.forexjournal.co.in/archive/volume-12/ijeer-120233.html

1. INTRODUCTION

The advancement of planar antenna technology has undergone significant and extensive enhancements over the past fifty years, serving as a crucial component in the design of wireless communication systems. However, the growing need for distinctive mobile communication systems in recent times has presented antenna designers with several new technological challenges, mostly stemming from additional non-standard performance criteria. Examples of communication systems that are portable and need establishing connections with satellites in remote locations may be found in the form of small mobile systems. These systems operate within the *C band*, specifically utilizing the uplink frequency range of 5.9 to 6.4 GHz. Consequently, there is a growing popularity of antennas that possess higher gain, smaller physical dimensions, superior directivity, and wider operating bandwidth. Consequently, the design of antennas is subject to far more rigorous and restrictive standards. The potential solution to address these requirements might be the implementation of the Quasi-Yagi antenna design. Modest and compact antenna designs can see a notable enhancement in gain and directivity with its use. Consequently, several research endeavors are now being conducted on Quasi-Yagi antennas [1]-[5].

The Quasi-Yagi antenna was developed as a derivative of the classic Yagi-Uda antenna. Yagi antennas are often employed to provide significant gain in a very straightforward configuration. The antenna was created in 1928 by Professors H. Yagi and S. Uda. [6]. Because of its low cost of construction, rapid feeding, excellent directivity, and high gain performance, the Yagi antenna has a wide range of applications in military and commercial applications. The primary drawbacks of any ordinary Yagi antenna are its relatively large size, restricted band (5%), and tuning complexity. As a result, the antenna's uses were limited [7]. Many studies have been conducted to find ways to get rid of these problems and use the Yagi antenna in the microwave range. As a consequence of merging the microstrip radiator technology with the Yagi-Uda array concept, which Huang initially described in 1991, a novel antenna construction is developed [8]. Nonetheless, Qian and colleagues [9] proposed the first printed quasi-Yagi-Uda antenna in 1998, and it has remained a key topic in today's research activity since then. The quasi-Yagi-Uda antenna combines the versatility of microstrip technology with the exceptional radiation properties of the Yagi-Uda antenna.

Several Quasi-Yagi antenna studies have been undertaken to enhance and/or optimize bandwidth, with the majority of them to raise the effective bandwidth. [9] proposes a 17% relative bandwidth transition from microstrip to coplanar strip (MS-to-CPS). Besides, the transition from a "coplanar waveguide to a coplanar strip (CPW to CPS)" defined by Ding et.al. in [10] may ignite the odd-mode electric field at the CPS line through the CPW feeding line. The antenna may operate at many frequencies at the same time. Providing 1800 phase delay might

FOREX Publication
Open Access | Rapid and quality publishing
International Journal of Electrical and Electronics Research (IJEER)
Research Article | Volume 12, Issue 2 | Pages 581-589 | e-ISSN: 2347-470X

also ignite the odd mode at the CPS line [11]. Nowadays, a microstrip line or a simple CPW with no transition structure is also utilized to directly imitate the Yagi-Uda antenna's feeding structure [12]. An octagon microstrip Yagi antenna [13] can obtain 15.97% bandwidth very recently. The research works in [14] and [15] achieved approximately 27.8% and 70.8% bandwidth, respectively. In [16], a 20.5% bandwidth was used in the construction of the top-hat monopole Yagi antenna.

The utilization of huge ground plates as reflectors is a recurring theme in the aforementioned study. These antennas often have huge diameters as a result, making them useless for array assembling and antenna downsizing. Reducing the total antenna size while boosting the directivity in the end-fire direction is therefore a difficult task. The size of the Yagi antenna has already been reduced using a variety of methods, including shrinking the area of the feeding network [17], substituting artificial transmission lines (ATLs) for radiating components [18], and changing the parabolic reflector [19]. Nevertheless, if a feeding system without a sizable ground plate can be created, the size and complexity can be significantly decreased [20].

A common characteristic in the above-mentioned research is that large ground plates are used as reflectors. As a result, these antennas usually have large size and are unbeneficial for antenna miniaturization as well as array composing. Thus, the challenge lies in reducing the overall antenna size while increasing the directivity to the end-fire direction. If a feeding structure without a large ground plate can be designed, the size and complexity can be greatly reduced.

Microstrip antennas feature a wide beam and low bandwidth. Radiation hits the antenna's broadside instead of the end fire needed for this investigation. These features may cause problems for unidirectional high-gain antennas with strong directivity. To alter bandwidth, use many antenna arrays with different resonance frequencies. However, this hampers design and manufacture. Slots are another typical antenna bandwidth-changing method. Vivaldi, moving, and linearly tapered slot antennas (LTSA) are also used, but they are larger.

This research uses C-band satellite communication. The first used for satellite communication was the C-band. However, terrestrial microwave communications use the same frequency, making the band busy. Current wireless radio networks may damage C-Band. Interferences can be reduced with pricey microwave filters or a narrow beam antenna setup. The C band has advantages including lower rain fade noise and cheaper bandwidth. Similar studies using the FR4 substrate yielded little gain and directivity. Rogers dramatically boosts gain and directivity in this study. This project will remove the constraints and construct a microstrip antenna with a narrow beam width within a bandwidth for C band (5.9–6.4 GHz) communications [21].

The paper is organized as follows: *section 1* provides the introduction of Quasi-Yagi antenna and the related works; *section 2* discusses the antenna design and dimension. The information regarding the fabrication method and the tools and technologies required to construct the antenna is presented in *section 3*. *Section 4* provides the results and discussions and finally, *section 5* concludes the paper.

2. ANTENNA DESIGN AND DIMENSION

This section describes the material selection process as well as the antenna dimension calculations. Substrate selection is the first and one of the most vital tasks of designing and fabricating an antenna. The antenna's performance depends heavily on the type of substrate used as its dielectric constant and thickness; both factors highly influence the antenna's bandwidth. The desired antenna in this work has a resonant frequency of 6.2 GHz with a specified bandwidth. It occupies the uplink C band satellite spectrum (5.9 GHz to 6.4 GHz). For this research, the Rogers 3003 substrate [22] is used with a relatively low dielectric constant of $\varepsilon_r = 3$ and thickness of 1.52 mm. the substrate has copper cladding on both sides with a copper thickness of 0.035mm. This substrate has a lower dielectric constant than the less expensive FR4 substrate. This lower dielectric constant can be expected to provide better gain and directivity for the Quasi Yagi antenna than one that uses an FR4 substrate.

The resonant frequency (f_c) is chosen at 6.2 GHz. The wavelength can be found from $\lambda_0 = \frac{c}{f_c}$, that is $\lambda_0 = 48.33\ mm$ where $c = 3 \times 10^8\ ms^{-1}$. The substrate used in the design has a dielectric constant of $\varepsilon_r = 3$. So, we can calculate the guided wavelength as $\lambda_g = \frac{\lambda}{\sqrt{\varepsilon_r}}$. That is, $\lambda_g = \frac{48.38}{\sqrt{3}}\ mm = 27.93\ mm$.

Figure 1 depicts the basic design schematics of the modified quasi-Yagi antenna. The traditional Yagi-Uda antenna, which consists of four primary components, is where the antenna construction is originated from:

1. The feeding part contains the feedline quarter, wave transformer, T-junction, balun, and the Coplanar Strip lines (CPS).
2. The second part is the driven elements which in this instance are the driven dipole (*λ/2*) elements.
3. The third part is the directors used for end-fire radiation and the high directivity.
4. The fourth part is the reflector. The truncated ground serves as the reflector.

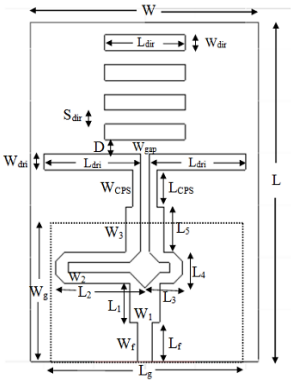

Figure 1. Design Schematics

FOREX Publication
Open Access | Rapid and quality publishing
International Journal of Electrical and Electronics Research (IJEER)
Research Article | Volume 12, Issue 2 | Pages 581-589 | e-ISSN: 2347-470X

The feeding part aims to transmit energy from the microstrip line to the Coplanar Strip lines and to the driven dipoles. The feedline calculations are made with the assumption of 50-ohm input impedance. Using the following equations, the feed line's width is matched to this input impedance.

If $\frac{W}{H} < 1$ then,

$$\varepsilon_{eff} = \frac{\varepsilon_r+1}{2} + \frac{\varepsilon_r-1}{2}\left[\frac{1}{\sqrt{1+12\left(\frac{H}{W}\right)}} + 0.04\left(1-\left(\frac{W}{H}\right)\right)^2\right] \quad (1)$$

$$Z_0 = \frac{60}{\varepsilon_{eff}} ln\left[8\left(\frac{H}{W}\right) + 0.25\left(\frac{W}{H}\right)^2\right] \quad (2)$$

But, if $\frac{W}{H} > 1$ then,

$$\varepsilon_{eff} = \frac{\varepsilon_r+1}{2} + \frac{\varepsilon_r-1}{\sqrt[2]{1+12\left(\frac{H}{W}\right)}} \quad (3)$$

$$Z_0 = \frac{120\pi}{\sqrt{\varepsilon_{eff}}\left[\frac{W}{H}+1.393+\frac{2}{3}ln\left(\frac{W}{H}+1.444\right)\right]} \quad (4)$$

Here, the substrate thickness H =1.52 mm and assuming $\frac{W}{H} > 1$, we can calculate the feedline width from *eq. (3)* and *eq. (4)*. The characteristic impedance of a quarter-wave long transformer can be calculated by the *equation (5)*

$$Z_1 = \sqrt{Z_0 R_L} \quad (5)$$

where Z_0 is the source impedance (50Ω), and R_L is the load impedance, whose value is determined by the T-junction circuitry. After getting the value of RL, characteristic impedance can be determined.

Table 1 lists the proposed compact unidirectional Quasi-Yagi antenna's optimum dimensions.

Table 1: Improved compact unidirectional Quasi-Yagi antenna dimensions

Parameter	Antenna element	Length in mm
W	Substrate width	45
L	Substrate length	60
W_g	Ground width	27.54
L_g	Ground width	33.42
W_f	Width of the feedline	3.3
L_f	Length of the feedline	6
L_{cps}	Length of CPS	5
W_{cps}	Width of CPS	1.5
W_{gap}	Width of gap	1.41
L_{dri}	Length of drivers	15.38
W_1	Width of Quarter wave	6
L_1	Width of Quarter wave	5
L_2	Length of left arm	10.61
L_3	Length of right arm	5.77
L_4	Width T junction	6
W_2	Width of arms	2
Wdri	Width of drivers	3.3
L_{sep}	Separation between directors	2.7
L_{dir}	Director lengths	13.55

3. FABRICATION AND MEASUREMENT PROCESS

3.1 Fabrication

The process of fabrication requires great attention to detail and offers little room for error, as even little deviations from the computer-simulated design can lead to significant discrepancies between experimental and simulated outcomes. Hence, the antenna was formulated and enhanced to function as a high gain antenna with notable directivity at a resonant frequency of 6.2 GHz within the Computer Simulation Technology (CST) Studio Suite. *Figure 2* illustrates the sequential procedures entailed in the manufacture of the antenna.

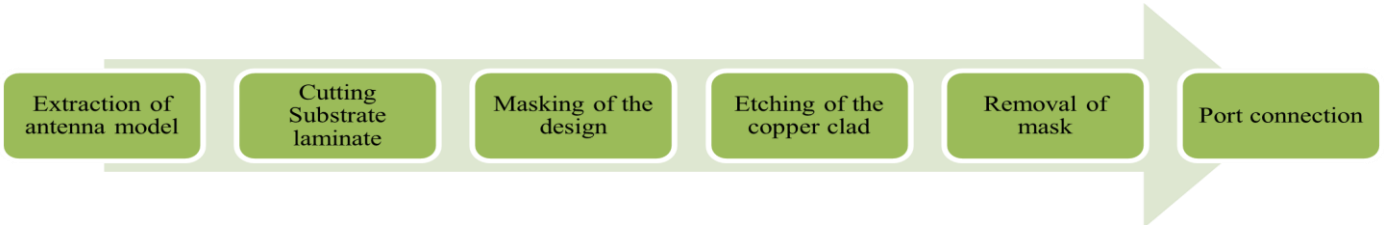

Figure 2. Fabrication process

The antenna was modeled and optimized in the CST Studio Suite. The antenna model can be extracted from the CST Studio Suite as a DXF file. The DXF format is chosen to get accurate scaling of the model. A 3D Laser Cutter is the best tool to cut a laminate precisely. But due to reactions of copper with the laser, the Rogers 3003 laminate is shaped by an electric saw machine. We need to print the antenna prototype on the substrate to create a mask for the copper clad. Due to the limitation of the laboratory facility, the design is manually printed on the laminates. The design traces were printed accurately and then

FOREX Publication
Open Access | Rapid and quality publishing
International Journal of Electrical and Electronics Research (IJEER)
Research Article | Volume 12, Issue 2 | Pages 581-589 | e-ISSN: 2347-470X

used to mask the laminates. The copper under the mask will remain on the substrate; the remaining copper clad will be etched off. The next step is to etch the copper clad from the laminate. We used the liquid lithography method to etch the copper. First, the laminates are soaked in a solution of Iron Chloride III (*Figure 3a*). Copper metal is easily dissolved by the FeCl3 solution. Electronics utilize it as a PCB etchant. FeCl3 has two potential uses as an etchant: Two powerful complexing agents for copper (II) ions are Cl- and Fe3+, respectively [23]. *Figure 3b* shows the laminates after the copper has been etched off.

(a)

(b)

Figure 3. (a) Soaking the masked laminates in the solution of $FeCl_3$; b) Laminates after the copper has etched off.

The paint utilized in the mask exhibits no reactivity with $FeCl_3$, although it does demonstrate solubility in organic solvents like ethanol. Subsequently, the laminate is subjected to an application of ethanol by spraying, followed by a rubbing process, therefore facilitating the removal of the paint layer and exposing the underlying copper material. The laminates without masks are depicted in *figure 4*.

The port connection represents the concluding stage in the production process of an antenna, followed by succeeding phases. The process of attaching a SMA (Sub Miniature version A) connector to the antenna's feedline is achieved using electrical soldering. The term "SMA connector" refers to a semi-precision coaxial RF connection. *Figure 5* illustrates the constructed antenna with a scale.

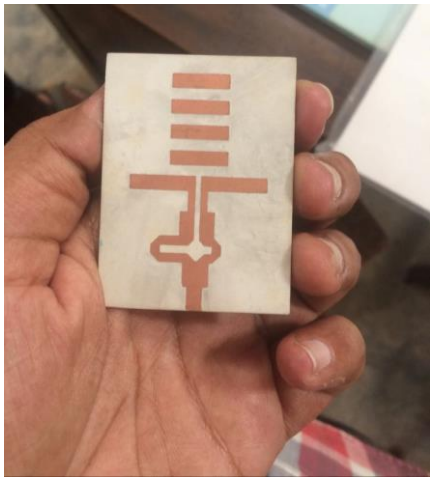

Figure 4. Laminate after removal of the mask

3.2 Testing and measurement

The antenna was tested in a laboratory of size 8m x 6m x 4m, with a floor and walls made of concrete. A Vector Network Analyzer (VNA) has been used to measure the antenna's return loss, bandwidth, VSWR, and smith chart. The radiation pattern was measured using Wave and antenna Training System (WATS-2002). VNA used in this experiment is of the model Rohde & Schwarz-8 Cable and Antenna Analyzer. After measuring, the data were imported from the VNA to a computer in a '.txt' file. MATLAB software was used to process this data and represent all the results. These results were compared with the simulation results from CST studio for analyzing the antenna's performance. The Rohde & Schwarz ZVH8 machine must be calibrated before using for measurements to ensure deviations do not occur. In this case, the Tx antenna was connected to port-1 and Rx antenna to Port-2 of VNA. Full 1port and Full 2 port calibrations were performed on VNA by R&S FSH-Z28 calibration kit [24] before using the VNA for measurements. For usage in the field, the R&S FSH-Z28 calibration standard is specifically made. It combines every calibration standard (open, short, 50-ohm load) required for DTF measurement and scalar or vector network analysis. For Full 2-Port Calibration, both test ports are calibrated for a complete set of measurements.

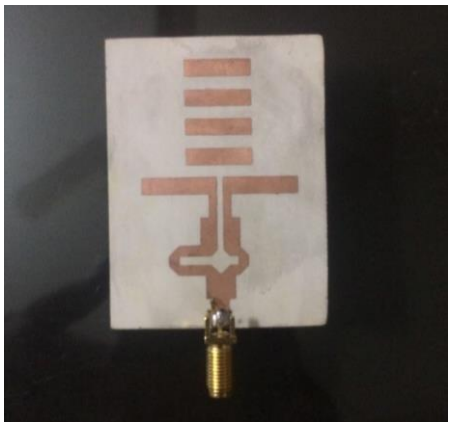

Figure 5. Antenna after port connection

FOREX Publication
Open Access | Rapid and quality publishing
International Journal of Electrical and Electronics Research (IJEER)
Research Article | Volume 12, Issue 2 | Pages 581-589 | e-ISSN: 2347-470X

For this work the forward transmittance(S_{11}) at the resonant frequency 6.2 was measured using the VNA while one of the antennas was used as the transmitter *Tx* and the other as the Receiver *Rx*. During this process, the receiver was rotated and controlled to account for the angular positions. A total of 100 measurements were taken, with each *Rx* rotation having 3.6^0 steps. Antenna rotation was done using WATS. By connecting two antennas to the VNA and then measuring the S_{21} at an operating frequency of 6.2GHz, we can measure the antenna's gain using the following equation.

$$G_R(db) = \frac{1}{2}\left[20\,log_{10}\left(\frac{4\pi r}{\lambda}\right) + S_{21}\right] \qquad (6)$$

4. RESULTS And DISCUSSION

This section centers on the results obtained from conducting laboratory tests on the constructed antenna, as well as the conclusions derived from simulating the 6.2GHz resonant antenna model. The CST Studio Suite software is used to create and simulate a quasi-Yagi antenna operating at a resonance frequency of 6.2GHz. The outcomes were subsequently extracted from the CST Studio Suite as text files and imported into MATLAB for the purpose of generating suitable visual representations. The antenna that was artificially constructed was also subjected to testing within the confines of the Microwave and Optical Fiber Communication Laboratory. The tests were conducted using the Rohde and Schwartz ZVH8 Vector Network Analyzer (VNA) instrument. The WATS 2002 system was used to achieve accurate rotation of the antennas.

4.1 Return Loss

At the frequency of resonance, the simulated return loss S11 exhibits a value of -36 dB, indicating a high level of power transmission efficiency. However, in practical scenarios, the antenna typically maintains a return loss of less than -10 dB. The objective is to determine the return loss S11 within the frequency range of 5.8GHz to 6.5GHz. The observed outcomes exhibited superior performance compared to the simulated outcomes, resulting in enhanced bandwidth and reduced minimum return loss. *Figure 6* provides a comparative analysis.

The bandwidth percentage can be calculated as:

$$BW = \frac{higher\ frequency, f_h - lower\ frequency, f_l}{resonant\ frequency, f_r}\%$$

$$BW = \frac{6.4\ GHz - 5.8\ GHz}{6.2\ GHz}\% = 8.87\%$$

At resonant frequency the simulated return loss S¬11 is -36 dB providing efficient transmission of power. The experimental findings indicate a resonance frequency of 6.24 gigahertz. At the frequency of resonance, the return loss S¬11 exhibits a value of -44 dB. The antenna sustains a signal attenuation of less than -10 dB.

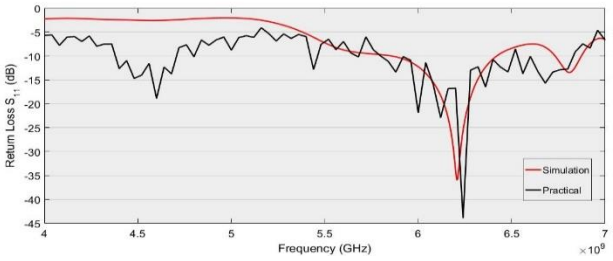

Figure 6. Comparison of simulated and practical return loss

4.2 Voltage Standing Wave Ratio (VSWR)

The Voltage Standing Wave Ratio (VSWR) of the antenna that has been designed exhibits consistent values across the whole frequency range, spanning from 5.85 to 6.4 GHz. Additionally, the Voltage Standing Wave Ratio (VSWR) at the central frequency (fc) of 6.2 GHz is measured to be 1.03, indicating a highly favorable impedance match for the antenna. Figure 7 presents a comparative analysis of the simulated and practical VSWR outcomes. Once again, there is a strong correspondence between the practical outcome and the simulated outcome. In the figure, it shows that the antenna has a VSWR<2 throughout the entire bandwidth (from 5.85 to 6.4GHz). VSWR at the center frequency fc (6.2 GHz), is 1.03, which ensures that the antenna has a very good match.

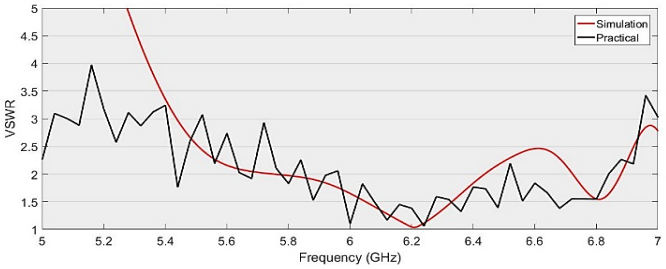

Figure 7. Comparison of simulated and practical VSWR

4.3 Gain

The simulated antenna has a notable gain of 9.17 dB while operating at its resonance frequency of 6.2 GHz. Electrically diminutive antennas, characterized by their small size relative to the wavelength of the frequency at which they operate, sometimes exhibit significant inefficiency. These antennas can possess antenna strengths lower than -10 dB, even when impedance mismatch loss is not taken into consideration. This outcome is really satisfactory.

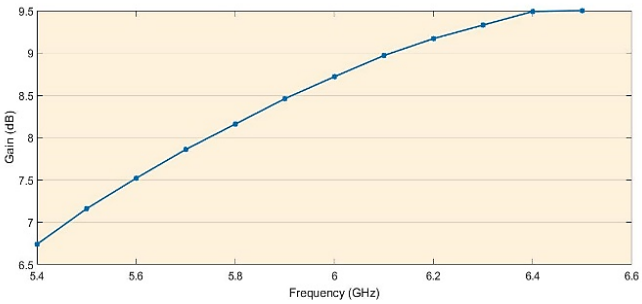

Figure 8. Gain vs frequency of the simulated antenna

FOREX Publication
Open Access | Rapid and quality publishing
International Journal of Electrical and Electronics Research (IJEER)
Research Article | Volume 12, Issue 2 | Pages 581-589 | e-ISSN: 2347-470X

Antennas with comparable characteristics operating at a frequency of 3.4 GHz, which were previously subjected to simulation in a laboratory setting, exhibited gains of merely 5.25 dB. According to the idea, the gain exhibits a positive correlation with frequency. The frequency response curve is depicted in *figure 8*.

4.4 Radiation Pattern

The Fairfield radiation pattern of the simulated antenna with respect to gain is depicted in *figures 9, 10, and 11*. The modelling results indicate a directivity of 9.38 dB at the 900 angles. The angular diameter of the radiation pattern is notably 57 degrees, which is significantly narrower compared to prior studies. Furthermore, it generates sidelobe levels with a magnitude of -16.9 dB. This feature guarantees that the design has the capability to function as a highly directional high-gain antenna. *Figure 9* gives the Polar far-field radiation pattern at 6.2 GHz for directivity.

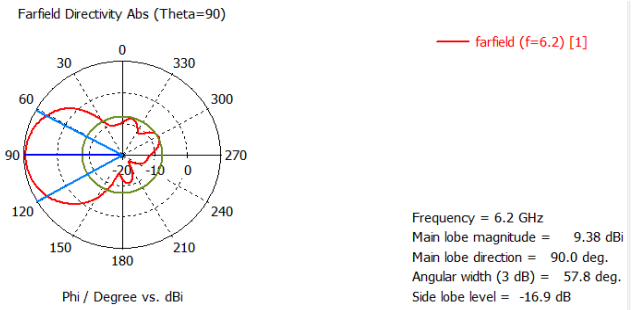

Figure 9. Polar radiation pattern for directivity abs *(simulation result)*

Figure 10 gives the Polar far-field radiation pattern at 6.2 GHz for gain. Empirically, it has been determined that the angular breadth of the half power beam is around 76 degrees, a value that somewhat exceeds the outcome obtained by simulation. The laboratory radiation pattern findings exhibit a similar configuration to the simulated radiation pattern, but with variations in the gain magnitude (see *figure 12*). The discrepancy arose due to the unavailability of an appropriate testing environment, specifically an anechoic chamber. Furthermore, it should be noted that the two antennas in question were not identical. These factors could potentially be attributed to the variation in the magnitude of gain. *Figure 11* gives 3D far-field representations.

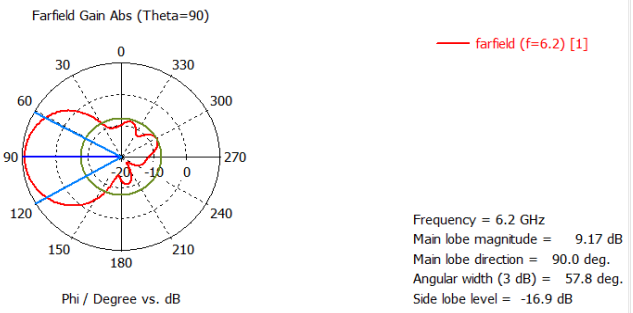

Figure 10. Polar radiation pattern for Gain abs *(simulation result)*

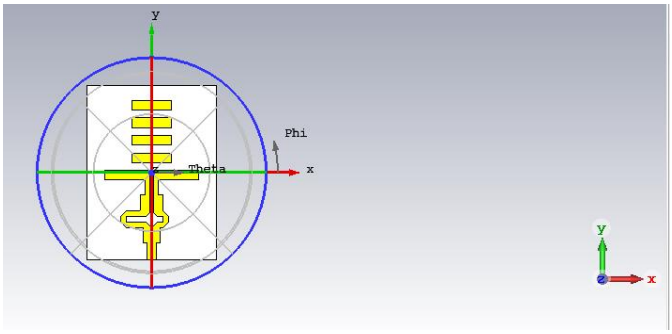

(a)

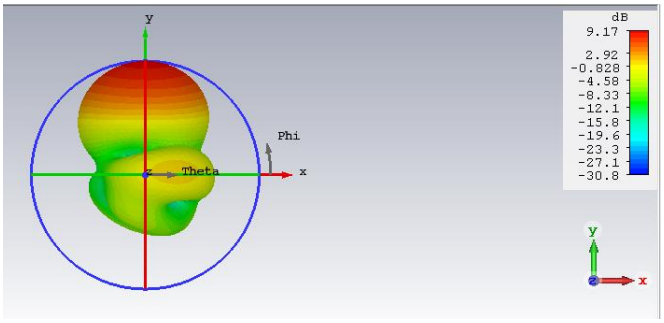

(b)

Figure 11. (a) Orientation of the antenna, (b) 3D radiation pattern of the antenna.

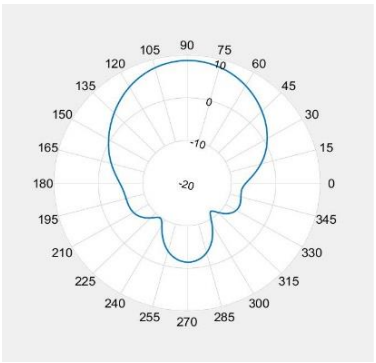

(a)

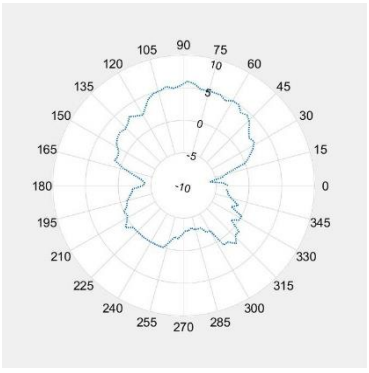

(b)

Figure 12. Comparison between (a) practical and (b) simulated radiated pattern

FOREX Publication
Open Access | Rapid and quality publishing
International Journal of Electrical and Electronics Research (IJEER)
Research Article | Volume 12, Issue 2 | Pages 581-589 | e-ISSN: 2347-470X

4.5 Radiation Efficiency

Efficiency takes into consideration the real losses incurred by a certain antenna design as a result of manufacturing flaws, surface coating losses, flaws, impedance mismatch, or any other issue.

So,

$$\text{Efficiency} = \frac{gain}{directivity} = G(dB) - D(dB)$$
$$= 9.17\ dB - 9.38\ dB$$
$$= -0.11\ dB$$
$$= 98.74\%$$

4.6 Impedance Measurement

The impedance of the manufactured antenna is determined by analyzing the Smith chart at a frequency of 6.24 GHz. The Vector Network Analyzer (VNA) is employed for the purpose of referencing the smith chart and obtaining impedance values. *figure 13* displays the results obtained from the laboratory test.

In *figure 13*, the impedance is observed to have a magnitude of 47.9 ohms and a phase angle of 4.51 degrees. The real component denotes the impedance value, which has been determined to be 48.11 ohms. The simulated impedance of 50 ohms is almost accurate.

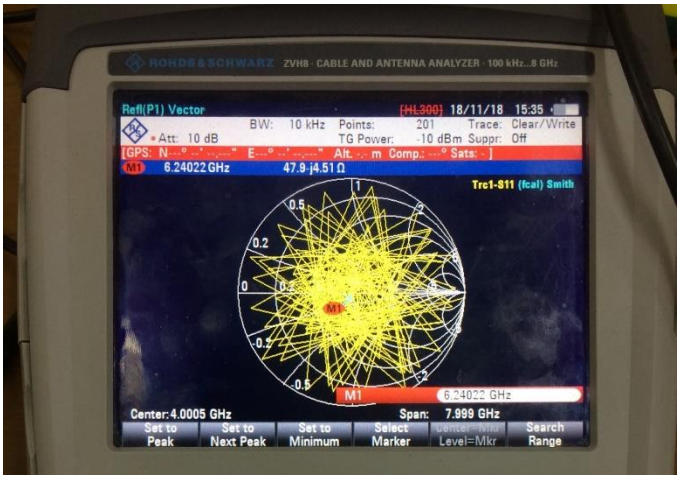

Figure 13. Impedance measurement

4.7 Radiation pattern of the fabricated antenna

The measurement of the radiation pattern is conducted *via* the Rohde and Schwartz Vector Network Analyzer (VNA) in conjunction with the WATS 2002 apparatus. Two almost identical antennas were employed to determine the S21 parameter of the antenna. Subsequently, this information was utilized to determine the antenna's gain. The data was subsequently graphed versus angular position using MATLAB. The lack of an anechoic chamber, as well as the absence of exact identical antennas, might lead to deviations from precise and accurate outcomes. The radiation pattern is provided below (Figure 14). The half power beam exhibits an angular width of 76 degrees. The observed outcome is moderately bigger than the simulated result.

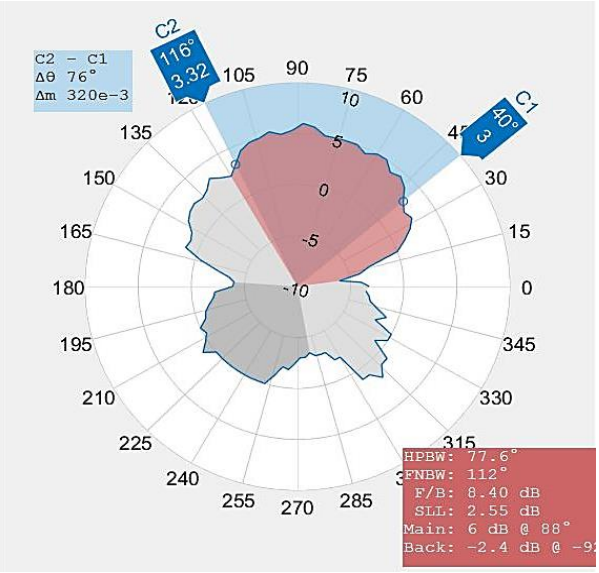

Figure 14. Fabricated antenna radiation pattern

Table 2 provides a synopsis of the overall comparison between the real-world and simulated findings that have been discussed above.

Table 2. Comparison analysis of the practical and simulated results

Parameters	Simulated results	Practical results
Resonant Frequency	6.2GHz	6.24 GHz
Bandwidth	5.85 to 6.4 GHz	5.8GHz to 6.5GHz
Bandwidth efficiency	8.87%	11.2 %
Return loss (S_{11})	-36 dB	-44dB
VSWR	1.03	1.05
Gain	9.17	6.35 dB
Angular width of half power beam	57.8	76 degrees
Main lobe direction	90	90 degrees
Impedance	50 ohms	48.11 ohms
Radiation	End fire radiation	End fire radiation

4.8 Comparative Results

The primary objective of this study is to design and develop an antenna with a high-gain and high-directivity operating at a frequency of 6.2 GHz. The findings obtained from simulating and fabricating the antenna demonstrate the successful achievement of the stated objectives. An end-fire radiation pattern was seen, accompanied by a high gain of 9.17 and directivity of 9.38.

Previous studies conducted at a frequency of 6.2 GHz were unable to achieve a gain of this magnitude. In their study, Sun Liling et al. [25] achieved a gain of 8.4 dB while maintaining low directivity by the utilization of a Butterfly-Shaped Wideband Microstrip Patch Antenna. In contrast, previous research [26] demonstrated an improvement of 2.8 dB at

International Journal of Electrical and Electronics Research (IJEER)
Research Article | Volume 12, Issue 2 | Pages 581-589 | e-ISSN: 2347-470X

frequencies of 6 GHz. In a study conducted in 2011, it was observed that a different work achieved a gain of 6 decibels (dB) at a frequency of 6.2 gigahertz (GHz), accompanied by a return loss of -27 dB [27]. In the year 2017, a P-shaped microstrip patch antenna operating in a tri-band configuration was developed, whereby one of the three frequencies utilized was 6.2 GHz. The recorded measurement exhibited an increase of 3.03 decibels [28]. A comparison table for the previous works is included in *Table 3*.

Table 3. Comparison with the existing literature

Corresponding work	Resonant Frequency (GHz)	Return loss (dB)	Gain (dB)
[25]	6.2	-30	8.4
[26]	6	-27	2.8
[27]	6.2	-27	6
[28]	6.2	-33.2	3.03
[29]	5	-32	8
This work	6.2	-44	9.17

5. CONCLUSIONS

A unique quasi-Yagi antenna with high gain and good directivity was simulated and fabricated in this work. This study aimed to design a compact 6.2 GHz antenna with excellent gain and strong directivity. A thorough review of technological solutions and their budgetary viability for our laboratory was done before starting antenna design. A detailed review of related antenna literature was then done to identify areas for improvement. The antenna was then designed in CST Studio Suite. After design, our lab tools were used to build the antenna. A Vector Network Analyzer (VNA) and Wave and Antenna Training System tested the antenna thoroughly. These experiments examined return loss, bandwidth, gain, impedance, and radiation pattern. The simulated and built antennas were then compared. There are several research opportunities in this field. Array multiple Quasi Yagi antennas for multiband applications may be investigated in the future. With 3D printers and laser cutters, antennas can be made precisely to design. All measurements were done in accessible labs. Anechoic chamber tests of this antenna improve data dependability and enable further investigation.

REFERENCES

[1] V. G. Kasabegoudar and S. Shirabadagi, "Quasi Yagi antennas for the state of the art applications," *Int. J. Eng. Trends Technol.*, vol. 70, no. 4, pp. 1–14, 2022.

[2] Y. Chen, J. Shi, K. Xu, L. Lin, and L. Wang, "A Compact Wideband Quasi-Yagi Antenna for Millimeter-Wave Communication," *IEEE Antennas Wirel. Propag. Lett.*, 2023.

[3] A. Kumar, E. Easha, D. Sarkar, and G. Banerjee, "A compact quasi-Yagi antenna for FMCW radar-on-chip-based through-wall imaging," *Int. J. Microw. Wirel. Technol.*, pp. 1–13, 2023.

[4] M. A. Haque, M. A. Zakariya, N. S. S. Singh, M. A. Rahman, and L. C. Paul, "Parametric study of a dual-band quasi-Yagi antenna for LTE application," *Bull. Electr. Eng. Informatics*, vol. 12, no. 3, pp. 1513–1522, 2023.

[5] M. Gupta and H. Kumar, "Compact, Broadband and High Gain Uniplanar Quasi-Yagi Microstrip Antenna for End-Fire Radiation," *IETE J. Res.*, pp. 1–10, 2023.

[6] H. Yagi, "Beam Transmission of Ultra Short Waves," *Proc. Inst. Radio Eng.*, vol. 16, no. 6, pp. 715–740, 1928, doi: 10.1109/JRPROC.1928.221464.

[7] K. Jiang, Q. G. Guo, and K. M. Huang, "Design of a wideband quasi-Yagi microstrip antenna with bowtie active elements," in *2010 International Conference on Microwave and Millimeter Wave Technology*, 2010, pp. 1122–1124, doi: 10.1109/ICMMT.2010.5525084.

[8] J. Huang and A. C. Densmore, "Microstrip Yagi array antenna for mobile satellite vehicle application," *IEEE Trans. Antennas Propag.*, vol. 39, no. 7, pp. 1024–1030, 1991, doi: 10.1109/8.86924.

[9] T. Itoh, "Microstrip-fed quasi-Yagi antenna with broadband characteristics," *Electron. Lett.*, vol. 34, no. 23, pp. 2194-2196(2), Nov. 1998, [Online]. Available: https://digital-library.theiet.org/content/journals/10.1049/el_19981583.

[10] Y. Ding, Y. C. Jiao, P. Fei, B. Li, and Q. T. Zhang, "Design of a Multiband Quasi-Yagi-Type Antenna With CPW-to-CPS Transition," *IEEE Antennas Wirel. Propag. Lett.*, vol. 10, pp. 1120–1123, 2011, doi: 10.1109/LAWP.2011.2170950.

[11] S.-J. Wu, C.-H. Kang, K.-H. Chen, and J.-H. Tarng, "A Multiband Quasi-Yagi Type Antenna," *IEEE Trans. Antennas Propag.*, vol. 58, no. 2, pp. 593–596, 2010, doi: 10.1109/TAP.2010.2041522.

[12] H.-D. Lu, L.-M. Si, and Y. Liu, "Compact planar microstrip-fed quasi-Yagi antenna," *Electron. Lett.*, vol. 48, no. 3, pp. 140–141, 2012.

[13] K. Quzwain, A. Ismail, and A. Sali, "Compact High Gain and Wideband Octagon Microstrip Yagi Antenna," *Electromagnetics*, vol. 36, no. 8, pp. 524–533, Nov. 2016, doi: 10.1080/02726343.2016.1236060.

[14] Y. Liu, H. Liu, M. Wei, and S. Gong, "A Novel Slot Yagi-Like Multilayered Antenna With High Gain and Large Bandwidth," *IEEE Antennas Wirel. Propag. Lett.*, vol. 13, pp. 790–793, 2014, doi: 10.1109/LAWP.2014.2318313.

[15] Z. Wang, X. Liu, Y. Yin, and J. Wu, "Dual-element folded dipole design for broadband multilayered Yagi antenna for 2G/3G/LTE applications," *Electron. Lett.*, vol. 50, no. 4, pp. 242–244, Feb. 2014, doi: https://doi.org/10.1049/el.2013.4146.

[16] Z. Hu, Z. Shen, W. Wu, and J. Lu, "Low-Profile Top-Hat Monopole Yagi Antenna for End-Fire Radiation," *IEEE Trans. Antennas Propag.*, vol. 63, no. 7, pp. 2851–2857, 2015, doi: 10.1109/TAP.2015.2427853.

[17] B.-Y. Park, M.-H. Jeong, and S.-O. Park, "A Miniaturized Microstrip-to-Coplanar-Strip Transition Loaded with Artificial Transmission Lines and 2.4-GHz Antenna Application," *IEEE Antennas Wirel. Propag. Lett.*, vol. 13, pp. 1486–1489, 2014, doi: 10.1109/LAWP.2014.2341552.

[18] Y. He and C. Liu, "Comments on 'Planar Artificial Transmission Lines Loading for Miniturization of RFID Printed Quasi-Yagi Antenna,'" *IEEE Antennas Wirel. Propag. Lett.*, vol. 13, p. 1815, 2014, doi: 10.1109/LAWP.2014.2387991.

[19] H.-C. Huang, J.-C. Lu, and P. Hsu, "On the size reduction of planar Yagi-Uda antenna using parabolic reflector," in *2015 Asia-Pacific Microwave Conference (APMC)*, 2015, vol. 1, pp. 1–3, doi: 10.1109/APMC.2015.7411775.

[20] I. Park, "Broadband CPS-fed Yagi-Uda antenna," *Electron. Lett.*, vol. 45, no. 24, pp. 1207-1209(2), Nov. 2009, [Online]. Available: https://digital-library.theiet.org/content/journals/10.1049/el.2009.1330.

[21] K. Dalal, T. Singh, and P. K. Singh, "A Low Profile Ultra-Wideband Antenna Design with Reconfigurable Notch-Bands for Wideband and Narrowband Applications," *Wirel. Pers. Commun.*, vol. 125, no. 2, pp. 1405–1423, 2022, doi: 10.1007/s11277-022-09611-3.

[22] K. Patidar, K. K. Yadav, and D. Yadav, "Performance Analysis of Substrate Integrated Waveguide with different Dielectric Materials for X-band applications," in *2020 4th International Conference on Electronics, Materials Engineering & Nano-Technology (IEMENTech)*, 2020, pp. 1–4, doi: 10.1109/IEMENTech51367.2020.9270069.

International Journal of
Electrical and Electronics Research (IJEER)
Research Article | Volume 12, Issue 2 | Pages 581-589 | e-ISSN: 2347-470X

[23] R. M. Atta, "Effect of applying air pressure during wet etching of micro copper PCB tracks with ferric chloride," *Int. J. Mater. Res.*, vol. 113, no. 9, pp. 795–808, 2022.

[24] H. R. Chowdhury, M. S. Hassan, and A. Ahmed, "Analysis of path loss characteristics in body area network for different physical structures," in *2016 9th International Conference on Electrical and Computer Engineering (ICECE)*, 2016, pp. 299–302.

[25] L. Sun, M. He, J. Hu, Y. Zhu, and H. Chen, "A butterfly-shaped wideband microstrip patch antenna for wireless communication," *Int. J. Antennas Propag.*, vol. 2015, 2015.

[26] M. N. Srifi, M. Meloui, and M. Essaaidi, "Rectangular slotted patch antenna for 5-6GHz applications," *Int. J. Microw. Opt. Technol.*, vol. 5, no. 2, pp. 52–57, 2010.

[27] A. P. S. Pharwaha and S. Rani, "Simulation and design of broad-band slot antenna for wireless applications," in *Proceedings of the world congress on Engineering*, 2011, vol. 2.

[28] S. Kaur, P. Sharma, and M. Singh, "Design of Tri Band P Shaped Microstrip Patch Antenna," *Int. J. Adv. Eng. Res. Dev.*, vol. 4, no. 10, 2017.

[29] B. Huang, M. Li, W. Lin, J. Zhang, G. Zhang, and F. Wu, "A Compact Slotted Patch Hybrid-Mode Antenna for Sub-6 GHz Communication," *Int. J. Antennas Propag.*, vol. 2020, p. 8262361, 2020, doi: 10.1155/2020/8262361.